The photo-dissociation of the pyrrole-ammonia complex - The role of hydrogen bonding in Rydberg states photochemistry

ARTICLE *in* PHYSICAL CHEMISTRY CHEMICAL PHYSICS · FEBRUARY 2012

Impact Factor: 4.49 · DOI: 10.1039/c2cp23849g · Source: PubMed

3 AUTHORS:

Shmuel Zilberg
Ariel University
66 PUBLICATIONS **1,123** CITATIONS
SEE PROFILE

Anat Kahan
Hebrew University of Jerusalem
11 PUBLICATIONS **101** CITATIONS
SEE PROFILE

Yehuda Haas
Hebrew University of Jerusalem
66 PUBLICATIONS **1,207** CITATIONS
SEE PROFILE

PCCP

Cite this: *Phys. Chem. Chem. Phys.*, 2012, **14**, 8836–8841

www.rsc.org/pccp

PAPER

The photo-dissociation of the pyrrole–ammonia complex—the role of hydrogen bonding in Rydberg states photochemistry†

Shmuel Zilberg,* Anat Kahan and Yehuda Haas

Received 4th December 2011, Accepted 23rd January 2012
DOI: 10.1039/c2cp23849g

The photochemistry of the pyrrole–ammonia cluster is analyzed theoretically. Whereas in neat pyrrole the dominant photochemical reaction is H-atom cleavage, recent experiments show that in pyrrole–ammonia clusters the major reaction is H-transfer to form the NH_4 radical (solvated by ammonia molecules in the case of large clusters) and the pyrrolyl radical. A mechanism involving the hydrogen-bonded Rydberg state is offered to account for these results and verified computationally. Two minima are located on the lowest excited singlet PES. Both of them are Rydberg states, one leads to the formation of NH_4 and pyrrolyl radicals, the other is connected to the $\pi\sigma^*$ state through a relatively high barrier, leading to a 3-body dissociation reaction to form a pyrrolyl radical, ammonia and an H-atom. The former is the energetically and statistically preferred one.

Introduction

Pyrrole is one of the most important building blocks of biological molecules. As some other aza-aromatic compounds, it is particularly suitable to survive under the solar radiation reaching the Earth. It is completely transparent throughout the near IR and visible part of the solar spectrum. Its electronic absorption spectrum starts at about 250 nm, and is very weak down to about 210 nm—a region in which the solar flux is negligible.[1,2] Furthermore, even after absorption, the molecule does not fluoresce or phosphoresce, having a very short lifetime that averts second order reaction. These facts show that very efficient radiationless processes cause rapid internal conversion to the ground state. In condensed phases it is essentially unreactive, whereas the isolated molecule was found to dissociate after irradiation in the deep UV.

After absorption in the weak bands between 250 and 215 nm, the only reaction is cleavage of the NH bond to form atomic hydrogen and the pyrrolyl radical. Absorption at shorter wavelengths leads in addition to ring isomerization and opening, yielding also products known from the thermal dissociation. Blank *et al.*[3] studied the pyrrole photo-dissociation under collision free conditions using 248 and 193 nm radiation. The products were followed using a time of flight mass spectrometer. At 248 nm the only products were the H atom and the corresponding radical. Three channels were observed—two of them (90% of the total) due to NH cleavage, and a minor channel involving CH bond cleavage. Of the two NH scission reactions, one leads to "fast" H atoms, the other to slower ones. Irradiation at 193 nm led to the same reaction channels, but in addition, heavier fragments were found such as HCN and cyclopropene. These channels were interpreted as being due to "hot" S_0 molecules formed by internal conversion. In the NH cleavage reactions, the "fast" channel was assigned to dissociation on the excited state surface, and "slow" one was due to statistical reactions from lower states such as S_0. The NH cleavage results were repeated and verified by several workers, in particular Ashfold and coworkers using higher resolution.[4,5]

Interpretation of these results was hampered for some time by controversies concerning the electronic excited states contribution to the known absorption spectrum.[1,2] Many states contribute, of which two are $\pi\pi^*$ valence states and the others Rydberg states leading to the 3s and 3p orbitals of the N atom. In addition, other states such as triplets and $\pi\sigma^*$ states are found in the same energy region, but not necessarily in the Franck–Condon (FC) region. The current consensus appears to be that the allowed transition at 210 nm is mainly due to a valence $\pi\pi^*$ transition, with some contribution from Rydberg states. The weak features at longer wavelengths are assigned to vibronically induced transition to "forbidden" valence and Rydberg states, with some contribution from triplet states. The lowest state in the FC region lies at 4.2 eV above S_0. It is revealed by the electron energy loss (EEL) spectrum.[6]

As the initially excited valence or Rydberg states are bound, a mechanism leading to the dissociation products was sought. Sobolewski and Domcke *et al.* offered a general mechanism that appears to satisfactorily explain the results.[7] Based on

Institute of Chemistry, The Edmond Safra Campus, Givat Ram, The Hebrew University of Jerusalem, 91904 Jerusalem, Israel. E-mail: shmuel@fh.huji.ac.il; Fax: +972-2-5618033; Tel: +972-2-6585848

† Electronic supplementary information (ESI) available: Complete active space MOs of the pyrrole–ammonia complex. See DOI: 10.1039/c2cp23849g

quantum chemical calculations they showed that at large NH separations, the πσ* state crosses the ground state. This situation holds for many other N and O aromatic molecules, notably phenol and indole. The details differ, depending on the relative order of the states in the FC region. In the case of pyrrole, the 3s Rydberg state is the lowest lying state. As the NH bond lengthens, the πσ* state becomes lower and it leads to the cleavage of the NH bond. A conical intersection between the πσ* state and the ground state may cause the system to cross the ground state, which is repulsive at these energies, but may live longer due to statistical vibrational energy redistribution (IVR) among all vibrational modes—leading to the "slow" component.[3] The direct reaction on the πσ* state is much faster and leads to the "fast" component.[3,7]

As mentioned above, pyrrole derivatives are in general photostable. In particular, the NH cleavage reaction is suppressed. Pyrrole clusters are obvious candidates for studying environmental effects on pyrrole photochemistry, as the interaction with the added species are weak compared to chemical bonding. Thus, the photochemistry of isolated pyrrole, surveyed above, appears as a good starting point.

Two papers dealing with the photolysis of pyrrole–ammonia complexes were recently published. In both, the most probable number of NH_3 molecules in the cluster was 3. David *et al.*[8] used a supersonic jet to prepare the clusters and a time-of-flight (TOF) mass spectrometer to probe the products. The laser pulses used for excitation were either nanosecond or picosecond long. The main products observed were $NH_4(NH_3)_m$ clusters. The ammonium radical (NH_4) is a rather short lived species (15 ps) when isolated, but is considerably stabilized by clustering with ammonia—the lifetime of the clusters is a few microseconds. Using a two-color pulsed extraction scheme, the authors showed that the observed cations ($NH_4^+(NH_3)_m$) arise from a long lived species. By varying the energy of the ionizing laser, they came to the conclusion that a H-transfer reaction occurs already in the pyrrole–$(NH_3)_m$ cluster, which is subsequently ionized. The reaction is a hydrogen transfer reaction inside the cluster, in which the H atom, initially bound to the pyrrole moiety, moves to one ammonia molecule. A new hydrogen bond, with the pyrrolyl radical as an acceptor, is formed, and is stable on the time scale of the experiment, as shown by delaying the ionizing (probe) laser with respect to the exciting (pump) one. It was found that the lifetime of the 1 : 1 cluster is about 10 ps. In larger clusters, longer lifetimes are recorded—13 and 24 ps for $m = 2$ and 3 respectively. The appearance times of the $NH_4(NH_3)_m$ clusters were found to be, within experimental error, the same as the decays of the parent clusters. The decay times of the ammonium radical clusters were quiet long—up to 1 μs.

Based on the relatively long lifetimes (10–30 ps) of the pyrrole–ammonia excited clusters, the authors[8] conclude that the impulsive mechanism that holds for the bare molecule does not apply to the clusters. On the basis of CASSCF calculations they offer a reaction route along the NH and NN coordinates. The reaction involves first an electron transfer to the solvent (ammonia molecules) followed rapidly by proton transfer. This results in an Excited State Proton Transfer (ESPT) mechanism.

Rubio-Lago *et al.*[9] used velocity map imaging to follow the same reaction. They observed a much smaller kinetic energy release than David *et al.*[8] They also found no evidence for a long lived (ps) intermediate. Therefore, their excited state hydrogen transfer (ESHT) mechanism is based on a reaction similar to that of bare pyrrole: a hydrogen atom is ejected at high velocity and is immediately trapped by the ammonia solvent molecules that form a solvated NH_4 radical. Thus, in contradiction to David *et al.*, they adopt the impulsive mechanism.

So, two different interpretations of experimental results in a focus of the proposed theoretical study: to compare on the *ab initio* level of calculations the impulsive (ESHT) *vs.* electronic (ESPT) mechanisms.

In this paper we present a new mechanism that accounts for the formation of the NH_4 radical (the discussion is all couched in terms of the adiabatic states). It is shown that a hydrogen bonded complex between a Rydberg state of the NH_4 radical and the pyrrolyl radical crosses the ground state of the complex, forming the observed ammonium radical product. High level CASSCF calculations of the pyrrole–ammonia complex support the mechanism that involves a couple of new pathways leading to the ammonium radical, including a triplet channel. We show that the impulsive channel appears to be less preferred compared to the 2-body dissociation route. The CASSCF calculations are presented for the pyrrole–ammonia 1 : 1 cluster (not studied experimentally) since the basic physics can be deduced from its properties, but, of course, the solvation of NH_4 by the $(NH_3)_x$ cluster could be an additional stabilization factor.

The physical aspects of H-bonding on the Rydberg state photochemistry have to be considered in the framework of general H-bonding in electronic excited states.[10]

Computational results

Extensive CASSCF calculations were carried out on the ground state (GS), the two lowest singlet states and the lowest triplet state of the H-bonded complex between pyrrole and ammonia. The CASSCF[11] methodology as implemented in the PCGAMESS[12] program suite has been used to study the ground-state and excited states and also their cation-radical. Ten orbitals were included in the active space of the CASSCF calculations—six occupied orbitals (three π and three σ MOs) and four unoccupied ones (two π*, one σ* and 3s Rydberg MO); the orbitals are shown in Scheme S1 (ESI†). The aug-cc-pVDZ basis set was used for all calculations. The procedure for locating symmetry allowed conical intersections is based on a method developed by Dick.[13]

All structures were optimized on the CASSCF level; single point CASMP2 calculations were performed for all of them. The results are summarized in Table 1.

The H-bond in the PyrH$\cdots$$NH_3$ complex (I) is typical for the ground state N–H$\cdots$N fragment: ~2.2 Å (Fig. 1a), similar to previous calculations.[14] CAS calculations were performed under the imposed constraint of C_s symmetry—the pyrrole molecular plane was kept as a symmetry plane. This symmetry restriction allows distinguishing between the Rydberg states ($\pi \rightarrow 3s$, A″ symmetry) and the valence $\pi \rightarrow \pi^*$ of A′ symmetry. Rydberg ($3s/\sigma^* \leftarrow \pi$) states are dark states, but transition to the $\pi \rightarrow \pi^*$ state is allowed.[15] The products of the homolytic 3-body dissociation channel (II), pyrrolyl radical (Pyr), H atom and

Table 1 CAS(12e/10o)(CAS-MP2)/aug-cc-pVDZ results. Relative (eV) and absolute (a.u) energies of the Pyr–H···NH_3 in ground and excited states; N–H bond distances (r(N···H), Å)

State	CAS	CAS-MP2	r(PyrN···H)	r(H···NH_3)	Species
I (S_0,$1^1A'$)	0 (−265.16832)	0 (−265.99027)	1.020	2.248	PyrH···NH_3
II (S_0, $1^1A''$)	4.2	4.35	>3.5	>4.0	Pyr + H + NH_3
III (S_1, $1^1A''$)	4.94	4.73	1.080	1.692	[Pyr-H···NH_3]*$_{Ryd}$
IV (S_1, $1^1A''$)	4.13	4.06	2.006	1.026	[Pyr···H-NH_3]*$_{Ryd}$
V ($2^1A'$)	6.34	5.53	0.998	2.250	[Pyr-H···NH_3]$_{\pi\pi^*}$
VII;$^1A'/1^1A''$	4.32	4.24	>3.7	1.019	S_0/S_1
VII; ($1^1A''$)	5.78	5.10	2.15	1.484	S_1, TS
VIII$^1A'/1^1A''$	5.48	5.05	2.221	1.598	S_0/S_1

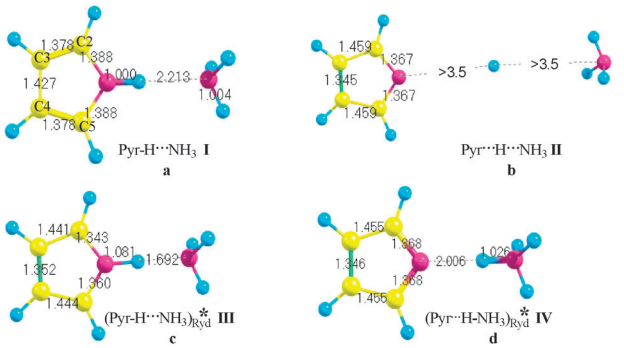

Fig. 1 (a) Ground state complex I; (b) products of 3-body dissociation, II; (c) S_1 π → 3s Rydberg excited state complex, III; (d) NH_4–Pyr Rydberg complex IV.

ammonia (Fig. 1b), are 4.35 eV (here and in the following discussion CAS-MP2 values are used) higher than ground state complex I.

The two lowest excited state minima of the pyrrole–ammonia complex are Rydberg state species III ($1^1A''$, π → 3s, Fig. 1c) and Pyr···H–NH_3 (IV) ($1^1A''$, π → 3s, Fig. 1d). Species III, which is in the Franck–Condon region, lies 0.4 eV higher than the 3-body dissociation limit. The second Rydberg state is the H-bonded complex between the pyrrolyl radical (Pyr) and the NH_4 radical. The lowest ππ* valence state is only the third excited singlet state S_3 (V).

The 3- and 2-body channels lead to two different $1^1A'/1^1A''$ crossings along N···N/N···H coordinates. For the 2- and 3- body reaction paths the N_{pyr}–H–N_{NH_3} coordinates were determined step by step from the reactant to product and all other coordinates were allowed to be optimized on the $1^1A''$ state using CAS. Calculations on the CAS/CAS-MP2 level of the $1^1A'$ state for each optimized geometry were also performed. Formation of the Pyr···NH_4 complex (IV) from III involves a small (0.1 eV) barrier. The structure of the conical intersection (CI) (VI) leading to the 2-body dissociation is very similar to the Pyr···NH_4 complex (IV). This is a sloped CI and it is only 0.18 eV higher than the Pyr···H–NH_3 intermediate (IV).

The lowest triplet $1^3A''$ is degenerate with the 2-body CI and is characterized by a fairly large spin–orbit coupling (SOC)—0.76 cm^{-1} with the $1^1A'$ component of this S_0/S_1 degeneracy. The 3-body dissociation channel has a high (for excited states) 0.75 eV barrier on S_1 (from the side of complex III, Table 1). S_1 crosses S_0 (VIII) near to this transition state (TS) (VII).

Two different cation-radical structures wherein the H-atom is connected to the pyrrole (IX, Fig. 2a) or to the ammonia (X, Fig. 2b) were located. The ionization potential of the initially formed complex I is 7.30 eV to IX; the H-shifted cation X is 0.15 eV above IX.

Discussion

Consider the electronic structure of the key species on the lowest excited singlet state (S_1) PES. The similar geometry found for the pyrrole moiety of the different S_1 species of the pyrrole–ammonia complex, S_1 Rydberg state III ($1^1A''$, π → 3s, Fig. 1c), isomeric S_1 Pyr···H–NH_3 complex IV ($1^1A''$, π → 3s, Fig. 1d) and also in both cationic structures IX and X, is a direct result of the π-system being populated by only 5 electrons. All structures, involving pyrrole HOMO excitation, undergo similar structural changes—a shortening of the central C3–C4 bond and a lengthening of C2–C3 (C4–C5) bonds (Fig. 1a). The same type of pyrrole distortion was reported also for the charge transfer state of the chemically bound phenyl-pyrrole[16] molecule, as one electron was promoted from HOMO. The energy of the electron removal is the same for the different excitations (from π-HOMO), and, consequently, the difference in the energies of species II–VII depends on the level of the *acceptor* orbital. π → π* excitation (S_3 and S_4) is higher than π → Rydberg (3s) (S_1 and S_2) by 0.6–0.8 eV (for detailed discussion of computed and experimental excitation energies of pyrrole see ref. 1, 15, 17–20).

The cation-radical of the parent complex I is a simple starting point for a model of the electronic excited states of the system upon promotion of π-HOMO electrons. This holds in particular for Rydberg[21] states. Our CAS calculations located two cation minima IX and X (Fig. 2) that differ in their H-bonding character. The H-shifted X is 0.22 eV higher than IX. These two cation isomers correspond to the two Rydberg state isomers, III and IV. Electron attachment to the cations IX and X leads to the different types of Rydberg species: III is a Rydberg state of the parent pyrrole plus NH_3,

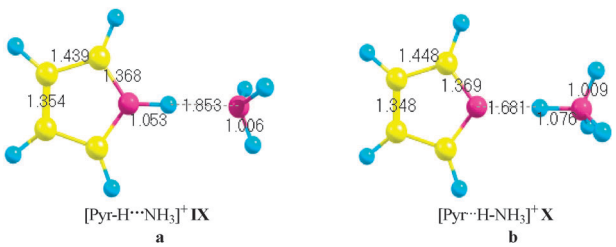

Fig. 2 (a) The pyrrole–ammonia complex $[Pyr–H···NH_3]^+$ cation IX. (b) The pyrrolyl–NH_4 complex $[Pyr···H–NH_3]^+$ cation, X.

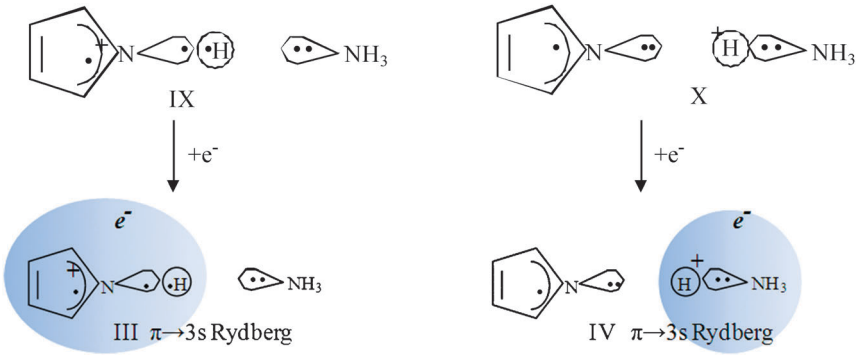

Scheme 1 Schematic presentation of the electronic structure's correlations between the isomeric cation-radicals IX and X, and their corresponding Rydberg species III and IV.

whereas IV is a complex between two radicals—pyrrolyl and Rydberg type NH_4 (Scheme 1).

Cation IX lies at $\Delta E_{IX-X} = -0.15$ eV below the isomeric H-shifted cation X. Electron attachment to the cations leads to considerable stabilization of H-transferred form IV relatively to III, $\Delta E_{III-IV} = 0.67$ eV. This result strongly supports the proposed electronic structure scheme (Scheme 1), because experimental results estimated the $\Delta E_{Rydberg\text{-}Cation} \approx 3.5$ eV (the first s-type Rydberg states of most molecules are found usually at ~25 000–32 000 cm^{-1} (*i.e.* ~3.5 eV) below the ionization limit[5]). The ionization potential (IP) of the NH_4 radical is ~4.5 eV according to experimental[22] and also theoretical estimation.[23] Consequently, electron attachment must stabilize IV *vs.* III by ~1 eV ($IP_{NH_4} - \Delta E_{Rydberg\text{-}Cation}$ = 4.5–3.5 = 1 eV), but taking into account $\Delta E_{VIII-IX} = -0.22$ eV, it leads to $\Delta E_{III-IV} \approx 0.8$ eV in excellent agreement with calculated values. Our CAS results agree on the whole with previous results of David *et al.*,[8] showing energy gap between III and IV: $\Delta E_{III-IV} \approx 0.6$ eV and a small barrier 0.1 eV between them (barrier from the side of the less stable isomer III).

The pyrrolyl radical acts as a spectator to the NH bond cleavage process as was observed experimentally in the bare pyrrole molecule.[24] The experimental dissociation limit of isolated pyrrole is 4.07 eV.[25] The calculated 3-body dissociation limit of the pyrrole–ammonia cluster is 4.35 eV (product II, Table 1). The process involves the rupture of the N–H bond and the loss of H-bonding. Comparison between these two values (4.07 *vs.* 4.35 eV) leads to the very plausible value of 0.28 eV for H-bonding stabilization of complex I.

Both cations IX and X have very strong (short) N···H hydrogen bonds—1.853 Å and 1.681 Å for IX and X, respectively. This behavior is also prominent in III ($r(H\cdots NH_3)$ = 1.692 Å) that correlates with the excited state Rydberg origin of the pyrrole moiety.

The Rydberg state minimum of the isolated pyrrole molecule shows shallow barrier (<0.1 eV) to N–H cleavage,[7,26] but strong H-bonding in Rydberg state complex III dramatically changes this picture, because the dissociation of III to products II (Pyr + H + NH_3) includes also the elimination of a strong H-bonding system. Calculations yield a 0.75 eV barrier on S_1 (VII, Table 1) for the 3-body dissociation of III. In the close neighborhood of TS VII the S_0/S_1 (VIII) crossing is also located (Fig. 3a). Thus, the 3-body dissociation channel is disfavored energetically with respect to the two-body one. In addition, it is also statistically a less preferable route. Thus the unusual strong H-bonding in Rydberg state species III could be a reason for suppression of the $\pi \rightarrow \sigma^*$ repulsive channel relatively to the isolated molecule's photodissociation and consequently, the 3-body dissociation impulsive mechanism[8,9] for the H-bonding complexes is less probable.

H-bonding in $[Pyr\text{–}H\cdots NH_3]^*_{Ryd}$ III is much stronger than in $[Pyr\cdots H\text{–}NH_3]^*_{Ryd}$ IV. The properties of the H-bonding in Rydberg-type IV are similar to those of the ground state parent complex I: (a) H-bond distance in IV 2.0 Å *vs.* 2.2 Å for I; (b) the computed H-bond energies are very similar for I ($E_{H\text{-}bond} = 0.27$ eV) and IV ($E_{H\text{-}bond} = 0.18$ eV). Comparison of the two Rydberg-type species III and IV allows different interpretations. David and coworkers proposed a mechanism,[8] which implies a reorganization of the charge after electronic excitation. Electron transfer is a starting point; a proton transfer is a following step, resulting in the formation of the $Pyr\cdots NH_4$ cluster. Here, an alternative interpretation is proposed: the Rydberg center shift (RCS) mechanism is based on the hypothesis that the Rydberg orbital is located on the pyrrole or ammonia components forming the cluster. The proton shift is escorted by the displacement of a 3s Rydberg orbital. As was pointed above (see Scheme 1 and the corresponding discussion), the shift of the Rydberg orbital from pyrrole to ammonia moieties is a driving force, providing stabilization of IV *vs.* III. The RCS mechanism is different from the excited state proton transfer (ESPT), and also from the excited state hydrogen-atom transfer (ESHT), but it can explain the transition to the 2-body dissociation funnel VI through $Pyr\cdots NH_4$ cluster IV.

NH_4 is a Rydberg type radical in its ground state.[27] Dissociation of NH_4 to (NH_3 + H) has a ~0.6 eV barrier at $R_{(N\text{–}H)} = 1.4$ Å, but the important physical feature is that NH_4 and (NH_3 + H) are isoenergetic.[28,29] Thus, the dissociation reaction starts from a 3s Rydberg state radical and ends with the electron localized on the 1s orbital of the H-atom. Our CAS calculations of pyrrole–NH_3 conform nicely with this interpretation: the products of the 2-body dissociation (Pyr + NH_4) IV and 3-body dissociation (Pyr + H + NH_3) II are isoenergetic on the CAS level. CAS-MP2 results show that the $NH_4\cdots$Pyr complex IV is 0.3 eV more stable than II. In spite of the similar energies, II is a ground state dissociation product, whereas IV is an excited state species—1.59 eV above the ground state ($1^1A'$) having the same structure. Our attempts to

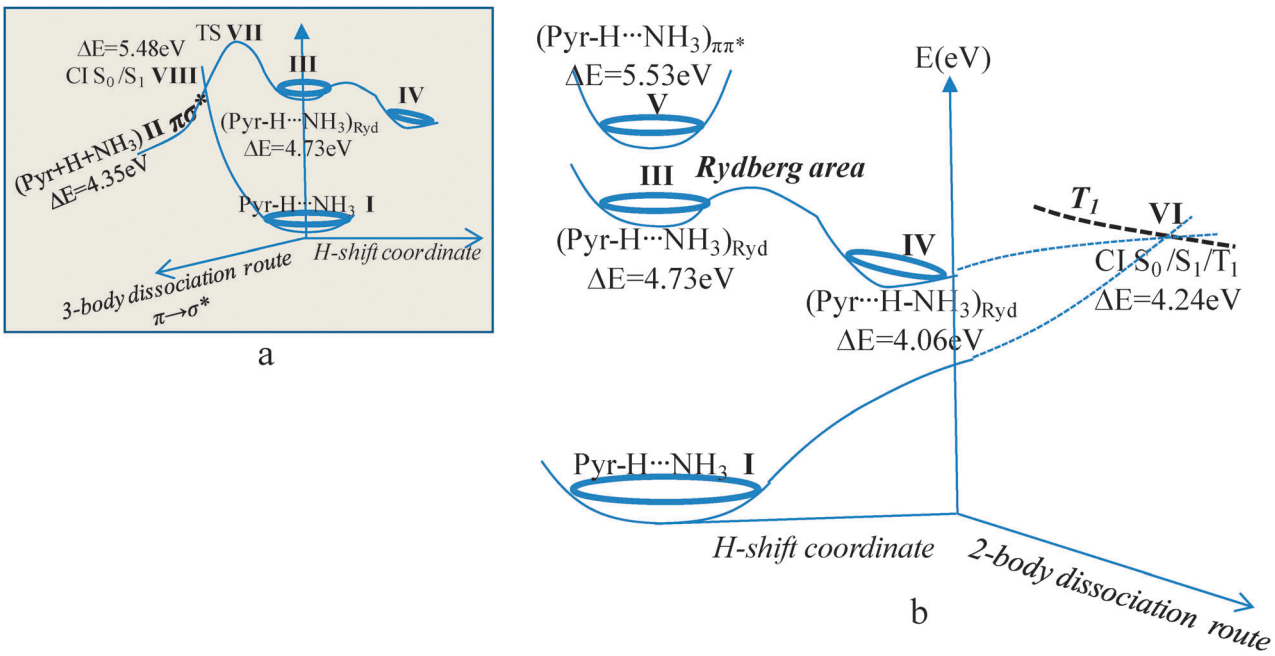

Fig. 3 Schematic energy level diagram of the pyrrole–ammonia H-bonding complex along: (a) 3-body dissociation coordinate, leading to the pyrrolyl radical, H atom and NH_3; (b) 2-body dissociation coordinate, leading to pyrrolyl and NH_4 radicals (CAS-MP2(12/10) results, please see Table 1).

localize singlet (Pyr···NH_4) on S_0 PES result in spontaneous H-transfer to the initial complex I.

The two H-bonding isomers III and IV on the S_1 PES are the key species for two different mechanisms of pyrrole–ammonia photodissociation: 3-body channel (Fig. 3a) and 2-body channel (Fig. 3b), respectively.

The NH_4 radical is of central importance in the interpretation of experimental findings on the pyrrole–ammonia photodissociation. A major goal of the theoretical model is revealing the significant 2-body dissociation channel, explaining its driving force and the electronic mechanism of NH_4 ejection. Production of a radical pair (Pyr + NH_4) by an electron-transfer induced proton-transfer mechanism was proposed early on, and the repulsion between NH_4 and the pyrrolyl radical was explained as due to the interaction between the pyrrolyl radical and the diffuse Rydberg-type electron cloud of NH_4.[8] Our results disagree with this explanation, because the complex (Pyr···NH_4) IV is calculated to be a global minimum on the S_1 PES. This is a bound excited state species whose barrier to dissociation to the radicals is 0.18 eV. No ground state analogue for (Pyr···NH_4) species IV was located and, consequently, internal conversion from S_1 complex IV to the ground state will lead to spontaneous H transfer to the initial complex I. The S_0 and S_1 states cross along the 2-body dissociation coordinate at an energy only 0.18 eV higher than that of the minimum of complex IV (Fig. 3). This sloped low-lying CI (VI) could provide an effective funnel for the return to the initial complex I (or to separated pyrrole and ammonia). Undoubtedly, the long distance between Pyr and NH_4 (>3 Å at CI VI) is a sufficient condition for the radical pair separation. Moreover this low lying CI coincides also with the lowest T_1. The triplet Pyr↑↑NH_4 pair is a repulsive complex that can explain the production of NH_4 on the ground state, provided that ISC is effective. The calculated spin–orbit coupling between the $^3A''$ and $^1A'$ states is 0.76 cm^{-1}, large enough to form an effective funnel to the triplet Pyr↑↑NH_4 pair. Intersystem crossing to the triplet in the CI region was proposed also for different systems[30] and observed experimentally for benzene.[31,32] The separation between the Pyr and NH_4 radicals can be further assisted by solvating NH_4 in a big $(NH_3)_x$ cluster. All three mechanisms are possible and dynamic calculations are needed for a quantitative analysis.

Our results compare well with previous pyrrole–ammonia experimental results.[8,9] The 2-body photodissociation channel, which results experimentally in the formation of $NH_4(NH_3)_m$ cluster is preferred over the 3-body dissociation. The "fairly long-lived intermediate state", whose lifetime is 10–30 ps, that David *et al.*[8] predicted from the experiment can be interpreted as IV, which is lower by 0.18 eV than VI and lower than III by 0.67 eV. Since a large release of kinetic energy and high velocities were found for the product (0.5 eV for the small cluster) David *et al.* concluded that the dissociation cannot be by an impulsive mechanism. We offer a new scheme (Scheme 1) that can explain the results based on the Rydberg cluster 2-body dissociation route as a funnel, using the RCS mechanism. The vibrational activity detected by Rubio-Lago *et al.*[9] also indicates an intermediate that has 1–1.5 eV available energy fraction channeled to kinetic energy, which fits well our calculated results: by comparison with the excitation energy (5.3–5.7 eV) the energy of the Rydberg cluster is of the order of 4–4.7 eV above the ground state. The existence of a well on the outgoing pathway is manifested by the relatively long-life of the product and by the rich vibrational activity.

Conclusions

(1) Two H-bonded isomers coexist on the S_1 PES of the pyrrole–ammonia cluster. Both are Rydberg type species and the electronic structure of these isomers is very similar to that

of the corresponding cations. In both cases, Pyr–H···NH_3 (III) and Pyr···H–NH_3 (IV) an electron is promoted from the pyrrole π-system to the Rydberg type orbitals. H-bonding strongly stabilizes the Pyr–H···NH_3 complex (III), but provides standard H-bonding stabilization for the H-shifted complex IV.

(2) The πσ* type photodissociation channel leading to formation of H-atoms, also exists, in principle, for the H-bonded complexes, but only as a 3-body dissociation. As far as we know, it has not been experimentally observed. Our model accounts for this fact as the extra stabilization due to H-bonding makes this route energetically less preferable than for the pyrrole parent isolated molecule. Another important factor is a statistical one, as 3-body reactions are low probability processes.

(3) The NH_4 containing complex (IV) is a bound excited state species. 2-Body dissociation of this complex to the pyrrolyl radical and NH_4 is possible on the ground state upon transition through the 2-body CI (VI) along the dissociation coordinate. This low-lying CI coincides also with the lowest triplet T_1 providing in principle an effective transition to the repulsive Pyr↑↑NH_4 triplet pair.

(4) According to the Rydberg center shift (RCS) mechanism the Rydberg orbital could be located on either the pyrrole or the ammonia components of the cluster. The proton shift is escorted by the shift of the Rydberg orbital, according to the new proton location. The RCS mechanism explains the transition to the 2-body dissociation funnel VI through the Pyr···NH_4 cluster IV in agreement with the experimental results of pyrrole–ammonia clusters.

Acknowledgements

Financial support from the DFG within the trilateral project Germany–Israel–Palestine Ma-515/22-2 is gratefully acknowledged.

Notes and references

1 M. H. Palmer, I. C. Walker and M. F. Guest, *Chem. Phys.*, 1998, **238**(2), 179–199.
2 P. Slavicek and M. Farnik, *Phys. Chem. Chem. Phys.*, 2011, **13**(26), 12123–12137.
3 D. A. Blank, S. W. North and Y. T. Lee, *Chem. Phys.*, 1994, **187**(1–2), 35–47.
4 B. Cronin, M. G. D. Nix, R. H. Qadiri and M. N. R. Ashfold, *Phys. Chem. Chem. Phys.*, 2004, **6**(21), 5031–5041.
5 M. N. R. Ashfold, G. A. King, D. Murdock, M. G. D. Nix, T. A. A. Oliver and A. G. Sage, *Phys. Chem. Chem. Phys.*, 2010, **12**, 1218–1238.
6 W. M. Flicker, O. A. Mosher and A. Kuppermann, *J. Chem. Phys.*, 1976, **64**, 1315–1321.
7 A. L. Sobolewski, W. Domcke, C. Dedonder-Lardeux and C. Jouvet, *Phys. Chem. Chem. Phys.*, 2002, **4**(7), 1093–1100.
8 O. David, C. Dedonder-Lardeux, C. Jouvet, H. Kang, S. Martrenchard, T. Ebata and A. L. Sobolewski, *J. Chem. Phys.*, 2004, **120**(21), 10101–10110.
9 L. Rubio-Lago, G. A. Amaral, A. N. Oldani, J. D. Rodriguez, M. G. Gonzalez, G. A. Pino and L. Banares, *Phys. Chem. Chem. Phys.*, 2011, **13**(3), 1082–1091.
10 G.-J. Zhao and K.-L. Han, *Acc. Chem. Res.*, DOI: 10.1021/ar200135h.
11 B. O. Roos, *Adv. Chem. Phys.*, 1987, **69**, 399–446.
12 A. A. Granovsky, *PC GAMESS version 7.0*, http://classic.chem.msu.su/gran/games/index.html.
13 B. Dick, *J. Chem. Theory Comput.*, 2009, **5**, 116–125. See also: B. Dick, Y. Haas and S. Zilberg, *Chem. Phys.*, 2008, **347**, 65–77.
14 (*a*) C. Rensing, H. Mäder and F. Temps, *J. Mol. Spectrosc.*, 2008, **251**(1–2), 224–228; (*b*) J. S. S. Toh, M. J. T. Jordan, B. C. Husowitz and J. E. Del Bene, *J. Phys. Chem. A*, 2001, **105**(48), 10906–10914; (*c*) J. Wu, A. Zhong, H. Yan, G. Dai, H. Chen and H. Lian, *Chem. Phys.*, 2011, **386**(1–3), 45–49.
15 B. O. Roos, P. Malmqvist, V. Molina, L. Serrano-Andres and M. Merchan, *J. Chem. Phys.*, 2002, **116**, 7526–7536.
16 S. Cogan, S. Zilberg and Y. Haas, *J. Am. Chem. Soc.*, 2006, **128**, 3335–3345.
17 D. J. Tozer, R. D. Amos, N. C. Handy, B. O. Roos and L. Serrano-Andrés, *Mol. Phys.*, 1999, **97**, 859–868.
18 M. Barbatti, M. Vazdar, A. J. A. Aquino, M. Eckert-Maksić and H. Lischka, *J. Chem. Phys.*, 2006, **125**, 164323–164327.
19 M. H. Palmer, I. C. Walker and M. F. Guest, *Chem. Phys.*, 1998, **238**, 179–199.
20 M. H. Palmer and P. J. Wilson, *Mol. Phys.*, 2003, **101**, 2391–2408.
21 G. Herzberg, *Annu. Rev. Phys. Chem.*, 1987, **38**, 27–56.
22 K. Fuke, R. Takasu and F. Misaizu, *Chem. Phys. Lett.*, 1994, **229**, 597–603.
23 F. Chen and E. R. Davidson, *J. Phys. Chem. A*, 2001, **105**, 10915–10921.
24 M. N. R. Ashfold, B. Cronin, A. L. Devine, R. N. Dixon and M. G. D. Nix, *Science*, 2006, **312**, 1637–1640.
25 B. Cronin, A. L. Devine, M. G. D. Nix and M. N. R. Ashfold, *Phys. Chem. Chem. Phys.*, 2006, **8**, 3440–3445.
26 A. L. Sobolewski and W. Domcke, *Chem. Phys.*, 2000, **259**, 181–191.
27 G. Herzberg, *Faraday Discuss. Chem. Soc.*, 1981, **21**, 165–173.
28 E. Kassab and E. M. Evleth, *J. Am. Chem. Soc.*, 1987, **109**, 1653–1661.
29 J. K. Park, *J. Chem. Phys.*, 1997, **107**, 6795–6803.
30 S. Cogan, Y. Haas and S. Zilberg, *J. Photochem. Photobiol., A*, 2007, **190**, 200–206.
31 D. S. N. Parker, R. S. Minns, T. J. Penfold, G. A. Worth and H. H. Fielding, *Chem. Phys. Lett.*, 2009, **469**, 43–47.
32 R. S. Minns, D. S. N. Parker, T. J. Penfold, G. A. Worth and H. H. Fielding, *Phys. Chem. Chem. Phys.*, 2010, **12**, 15607–15615.